International Journal of Electrical and Computer Engineering (IJECE)
Vol. 10, No. 5, October 2020, pp. 4522∼4533
ISSN: 2088-8708, DOI: 10.11591/ijece.v10i5.pp4522-4533

Fixed-time observer-based distributed secondary voltage and frequency control of islanded AC microgrids

Mohamed Ghazzali[1], Mohamed Haloua[2], Fouad Giri[3]
[1,2]Electrical Engineering Department, Mohammadia School of Engineers, Mohammed V University, Morocco
[3]Caen Automation Laboratory (LAC), Caen Normandie University (UNICAEN), UFR de Sciences, France

Article Info

Article history:

Received Oct 1, 2019
Revised Mar 14, 2020
Accepted Mar 26, 2020

Keywords:

Distributed observer
Fixed-time control
Microgrid
Secondary frequency control
Secondary voltage control

ABSTRACT

This paper deals with the problem of voltage and frequency control of distributed generators (DGs) in AC islanded microgrids. The main motivation of this work is to obviate the shortcomings of conventional centralized and distributed control of microgrids by providing a better alternative control strategy with better control performance than state-of-the art approaches. A distributed secondary control protocol based on a novel fixed-time observer-based feedback control method is designed for fixed-time frequency and voltage reference tracking and disturbance rejection. Compared to the existing secondary microgrid controllers, the proposed control strategy ensures frequency and voltage reference tracking and disturbance rejection before the desired fixed-time despite the microgrid initial conditions, parameters uncertainties and the unknown disturbances. Also, the controllers design and tuning is simple, straightforward and model-free.i.e, the knowledge of the microgrid parameters, topology, loads or transmission lines impedance are not needed in the design procedure. The use of distributed control approach enhances the reliability of the system by making the control system geographically distributed along with the power sources, by using the neighboring DGs informations instead of the DG's local informations only and by cooperatively rejecting external disturbances and maintaining the frequency and the voltage at their reference values at any point of the microgrid. The efficiency of the proposed approach is verified by comparing its performance in reference tracking and its robustness to load power variations to some of the works in literature that addressed distributed secondary voltage and frequency control.

Corresponding Author:

Mohamed Ghazzali,
Department of Electrical Engineering,
Mohammadia School of Engineers, Mohammed V University,
Ibn Sina Avenue, B.P. 765, Agdal, Rabat, Morocco.
Email: ghazzalimohamed1@gmail.com

1. INTRODUCTION

Microgrids are defined as electrical distribution networks, composed of distributed mainly renewable energy based power sources, called distributed generators (DGs), of loads and of energy storage systems, and managed autonomously from the main power grid [1, 2]. The concept of islanded microgrids emerged to coordinate the contradiction between the distributed nature of renewable energy power sources and the large electrical network. Microgrids require proper control to maintain the voltage magnitude and the frequency at their reference values.

Two main approaches were suggested for microgrids control: centralized and distributed control. Centralized control has been extensively used in literature for both AC and DC microgrids control [3–13] including secondary control [3–5] and power management [6–8] among others [9–13]. Distributed control is

a modern control approach developed as a natural solution for the naturally distributed systems as a more reliable control strategy, since the control is geographically distributed along with the system. It has applications in several fields including robotics [14–19], power electronics [20–24] and microgrid control [1, 25–30]. A distributed controller uses the informations of its neighboring components in addition to its local data to achieve regulation and reference tracking without having access to the reference itself. Thus, the system nonlinearities, parameters uncertainties and external disturbances are handled cooperatively at every component of the system, enhancing as a consequence the control efficiency. The data sharing feature of distributed control also increases the control system reliability as one component's failure is compensated by the others without hindering the control performance.

However, centralized control has several shortcomings. First, it requires heavy computational capacity as all the microgrid components are commanded by a single centralized controller. Thus, the control system implementation is financially expensive, which adversely affects its scalability. Centralized control also offers a single failure point as the micogrid control operations are conducted by one controller, which hinders the control system reliability. As for distributed control, asymptotic distributed secondary microgrid controllers has been suggested in literature [25, 27, 1, 29], however, disturbance rejection and reference tracking cannot be achieved in a finite-time due to the asymptotic convergence, and increasing the control gains makes the controller more sensible to external disturbances and parameters uncertainties and may destabilize the system instead of increasing its response speed. Furthermore, in [29] and [27] among others, the design procedure of the proposed control protocols requires a detailed non-linear model of the microgrids while, in practice, most of the microgrid parameters including line impedances, loads parameters and power demand are unknown. A few works proposed finite-time distributed secondary microgrid controllers [26, 28]. The settling-time is finite in this case, yet it depends on the systems parameters and initial conditions, and the mathematical relation between the control gains and the settling-time is not established. This means that the controller tuning can only be conducted manually by trials and errors and a automatic tuning algorithm can't be used in this case which hinders further the control performance.

To achieve better control performance than the existing centralized and distributed secondary microgrid controllers while obviating their shortcomings, this paper investigates a distributed observer-based secondary approach for frequency and voltage fixed-time control in AC islanded microgrids. The main contributions in this work are as follows:

(a) A fixed-time feedback observer-based controller is designed to achieve frequency and voltage reference tracking and disturbance rejection before the desired fixed-time irrespective to the microgrid initial conditions, parameter uncertainties and the unknown disturbances.
(b) The controller design is model-free,i.e., the microgrid topology, parameters, loads, or the transmission lines impedance are not required in the design procedure.
(c) Simple and straightforward design and tuning procedure.
(d) The proposed control law has a simple expression and therefore, it can be easily implemented and it does not require a hardware with high computational capacity. The reference tracking performance of the proposed control system and its robustness to load power variations is verified through a comparative simulation study with some of the works that addressed distributed secondary voltage and frequency control.

The rest of this paper is organized as follows. In Section 2., a detailed mathematical model of islanded microgrids is presented. Section 3. is devoted to the design of the proposed voltage and frequency secondary controllers. In Section 4., the comparative simulation study with some of the works that addressed distributed secondary control of microgrids is provided. Finally, the study is summarized and concluded in Section 5.

2. MATHEMATICAL MODEL OF AN ISLANDED AC MICROGRID

A comprehensive mathematical model of an islanded AC microgrid is presented in this section. It is required for the simulation study that will be conducted later. An accurate mathematical representation of a microgrid should include all the components with dynamics that define the behavior of each DG. Therefore for an islanded AC microgrid containing n parallel DGs with DC power sources, these components are as follows:

(a) The series RL filter.
(b) The shunt capacitor C_{ti} that attenuate the impact of high-frequency voltage harmonics of the local load.

(c) The step-up transformer ($Y - \Delta$) with transformation ratio m_i connecting the DG to the transmission line at the corresponding point of common coupling (PCCi) $i \in \{1, ..., n\}$
(d) The internal control loops of the voltage and the current of the voltage-source converter (VSC).
(e) The transmission lines modeled as RL series circuits to simulate both the resistive and the inductive behavior of power lines.

An example of a two DGs islanded microgrid in the $d - q$ frame can be seen in Figure 1.

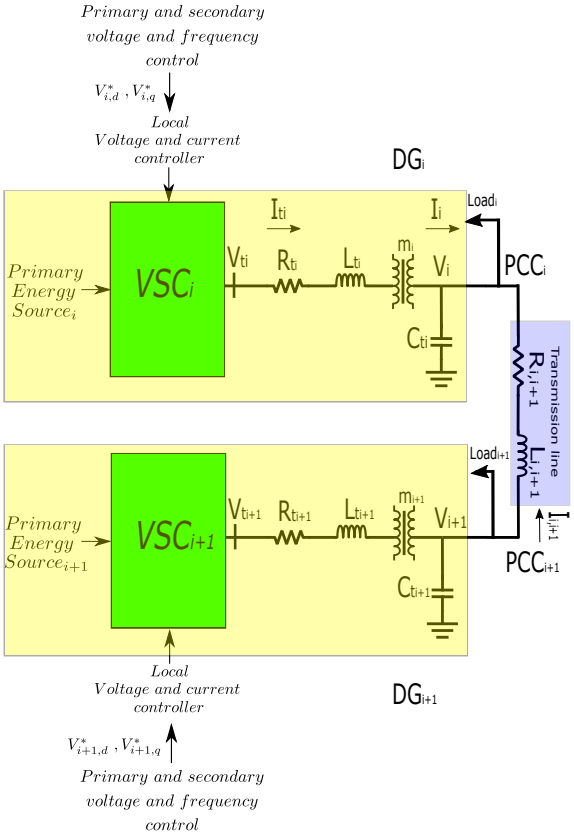

Figure 1. A two DGs islanded microgrid

A large signal non-linear model of DGi, $i \in \{1, ..., n\}$ is given as follows [3]:

$$
\begin{cases}
I_{i,d} = m_i I_{ti,d} - C_{ti}\dot{V}_{i,d} + C_{ti}\omega_i V_{i,q} \\
I_{i,q} = m_i I_{ti,q} - C_{ti}\dot{V}_{i,q} - C_{ti}\omega_i V_{i,d} \\
\dot{x}_i = A_i x_i + \sum_{j \in N_i} A_{ij} x_j + B_i u_i + D_i w_i \\
V_{ti,d} = V^*_{ti,d} \\
V_{ti,q} = V^*_{ti,q} \\
V^*_{ti,d} = -\omega_n L_{ti} I_{ti,q} + K_{pci}(I^*_{ti,d} - I_{ti,d}) \\
\quad + K_{ici} \int (I^*_{ti,d} - I_{ti,d}) \\
V^*_{ti,q} = \omega_n L_{ti} I_{ti,d} + K_{pci}(I^*_{ti,q} - I_{ti,q}) \\
\quad + K_{ici} \int (I^*_{ti,q} - I_{ti,q}) \\
I^*_{ti,d} = F_i I_{i,d} - \omega_n C_{ti} V_{i,q} + K_{pvi}(V^*_{i,d} - V_{i,d}) \\
\quad + K_{ivi} \int (V^*_{i,d} - V_{i,d}) \\
I^*_{ti,q} = F_i I_{i,q} - \omega_n C_{ti} V_{i,d} + K_{pvi}(V^*_{i,q} - V_{i,q}) \\
\quad + K_{ivi} \int (V^*_{i,q} - V_{i,q})
\end{cases}
\tag{1}
$$

Where $I_{i,d}$, $I_{i,q}$, $V_{i,d}$, $V_{i,q}$, $I_{ti,d}$, $I_{ti,q}$, $V_{ti,d}$ and $V_{ti,q}$ are the direct and the quadrature components of I_i, V_i, I_{ti} and V_{ti} in Figure 1. $x_i = \left(V_{i,d}, V_{i,q}, I_{ti,d}, I_{ti,q}\right)^T$ is the state vector. $u_i = \left(V_{ti,d}, V_{ti,q}\right)$ is the input and $w_i = \left(I_{Li,d}, I_{Li,q}\right)$ is the load current consumption considered as a know disturbance and an exogenous input to the system, for $i \in \{1, ..., n\}$. $\omega_i = 2\pi f_i$ is the i^{th} DG's output pulsation and f_i its output frequency. f_i control law will be defined in the next section. $\omega_n = 2\pi f_n$ is the nominal pulsation with $f_n = 50$ Hz the nominal frequency. The state-space matrices A_i, A_{ij}, B_{1i} and B_{2i} are defined in [31].

The microgrid communication network is modeled as an n-order weighted diagraph (directed graph) $G = (V, E)$ with $V = (v_1, v_2, ..., v_n)$ the set of nodes and $E \subseteq V \times V$ the set of directed edges. The weight $a_{ij} \geq 0$ associated with every edge is defined as follows

(a) $a_{ij} > 0$ if there is an edge from node j to node i. i.e., node i can receive informations from node j.
(b) $a_{ij} = 0$ otherwise.
(c) $a_{ii} = 0$ as self-loops are not allowed.

The adjacency matrix of the graph G is defined as $A = (a_{ij})_{i,j \in n \times n}$ and the Laplacian matrix as $L = D - A$ with $D = diag\{d_1, d_2, ..., d_n\}$, $d_i = \sum_{j=1}^{n} a_{ij}$.

3. THE PROPOSED VOLTAGE AND FREQUENCY CONTROL PROTOCOL

The droop-based voltage and frequency control for the i^{th} DG, $i \in \{1, ..., n\}$, is given by the following equations:

$$\begin{cases} V_{i,d}^* = u_{vi} - D_q Q_i, \\ V_{i,q}^* = 0, \\ \omega_i = u_{\omega i} - D_p P_i, \end{cases} \tag{2}$$

where u_{vi} and $u_{\omega i}$ are respectively the voltage and frequency control inputs to be designed. DGi generates the desired voltage reference, thererfore $V_{i,d}^* = V_{i,d}$ and $V_{i,q}^* = V_{i,q} = 0$. Thus, (2) becomes

$$\begin{cases} V_{i,d} = u_{vi} - D_q Q_i, \\ V_{i,q} = 0, \\ \omega_i = u_{\omega i} - D_p P_i, \end{cases} \tag{3}$$

Since the droop-control cancels the quadrature term of the voltage and DGi output voltage magnitude $V_{i,mag}$ satisfies $V_{i,mag} = \sqrt{V_{i,d}^2 + V_{i,q}^2}$, then control voltage amplitude is equivalent to controlling the output voltage direct term.

Differentiating the voltage and frequency droop equations yields

$$\begin{cases} \dot{V}_{i,d} = \dot{u}_{vi} - D_q \dot{Q}_i = z_{vi}, \\ \dot{\omega}_i = \dot{u}_{\omega i} - D_p \dot{P}_i = z_{\omega i} \end{cases} \tag{4}$$

where z_{vi} and $z_{\omega i}$ are the auxiliary control inputs. u_{vi} and $u_{\omega i}$ will be designed is the same way. Therefore to avoid redundancy, denote for the i^{th} DG u_i the voltage or frequency control input, $x_i \in \{V_{i,d}, \omega_i\}$ the output voltage $v_{i,d}$ or the pulsation ω_i and $x_0 \in \{V_0, \omega_0\}$ the reference pulsation $\omega_0 = 2\pi f_0$ or voltage amplitude. We also denote $z_i \in \{z_{vi}, z_{\omega_i}\}$ the auxiliary control input and $\gamma_i \in \{D_q Q_i, D_p P_i\}$ the power ratio. Thus, one can write

$$\dot{u}_i = z_i + \dot{\gamma}_i \ \ and \ \ \dot{x}_i = z_i \tag{5}$$

We propose the following fixed-time feedback-state auxiliary control z_i

$$z_i = \begin{cases} \dot{x}_0 - ke_1, For\ the\ leader\ DG\ (DG1) \\ \dot{\tilde{x}}_1^i - ke_i, For\ DGi\ (i \neq 1) \end{cases} \tag{6}$$

where k is the control gain and e_i is the i^{th} DG reference tracking error defined as follows:

$$\begin{cases} e_1 = \left(\mid x_1 - x_0 \mid^{1/2} + \mid x_1 - x_0 \mid^{3/2} \right) sign(x_1 - x_0), i = 1 \\ e_i = \left(\mid x_i - \tilde{x}_1 \mid^{1/2} + \mid x_i - \tilde{x}_1 \mid^{3/2} \right) sign(x_i - \tilde{x}_1), i \neq 1 \end{cases} \tag{7}$$

where x_0 is the reference state and $\tilde{x}_1^i$ is the estimation by DG$i, i \in \{2, ..., n\}$ of the state x_1 of the leader DG (designated DG1 in this paper). The estimation $\tilde{x}_1^i$ is provided by the distributed fixed-time observer designed as follows:

$$\begin{aligned} \dot{\tilde{x}}_1^i &= \alpha sign\big(\sum_{i=1}^{n} a_{ij}(\tilde{x}_1^j - \tilde{x}_1^i) + b_i(x_1 - \tilde{x}_1^i)\big) \\ &+ \beta\big[\sum_{i=1}^{n} a_{ij}(\tilde{x}_1^j - \tilde{x}_1^i) + b_i(x_1 - \tilde{x}_1^i)\big]^2 \end{aligned} \tag{8}$$

Where $\beta = \frac{\epsilon\sqrt{n}}{(2\lambda_m min(L+B))^{\frac{3}{2}}}$ and $\alpha = \epsilon\sqrt{\frac{\lambda_{max}(L+B)}{2\lambda_{min}(L+B)}}$. L is the Laplacian of the graph modeling the communication network defined in the previous section. $B = diag\{b_1, b_2, ..., b_n\}$ is the pinning gain matrix where $b_i = 1, i \in \{1, ..., n\}$ for the DGs having access to the leader DG 's state x_1, $b_i = 0$ otherwise. $\lambda_{min}(L + B)$ and $\lambda_{max}(L + B)$ are respectively the minimum and the maximum eigenvalue of $L + B$. If the observer is designed as in (8), the estimated state $\tilde{x}_1^i, i \in \{2, ..., n\}$ reaches the state x_1, i.e., $\tilde{x}_1^i = x_1$ before the fixed-time T_0 given as follows [32]:

$$T_0 \leq \frac{n\pi}{\epsilon} \tag{9}$$

u_i is designed in virtue of (5) and (6) as follows

$$u_i = \begin{cases} \int(\dot{x}_0 - ke_1 + \dot{\gamma}_1)dt, i = 1 \\ \int(\dot{\tilde{x}}_1^i - ke_i + \dot{\gamma}_i)dt, i \neq 1 \end{cases} \tag{10}$$

The following Lemmas are needed in the subsequent analysis.
Lemma 1 [33] Consider $y_1, y_2, ..., y_n \geq 0$, $0 < \alpha \leq 1$, $\beta > 1$. Therefore

$$\sum_{i=1}^{n} y_i^\alpha \geq \Big(\sum_{i=1}^{n} y_i\Big)^\alpha, \ \sum_{i=1}^{n} y_i^\beta \geq n^{1-\beta}\Big(\sum_{i=1}^{n} y_i\Big)^\beta \tag{11}$$

Lemma 2 [32] Consider the simple-integrator system

$$\dot{x} = g(t, x), \ x(0) = 0 \tag{12}$$

where $g : R_+ \times R^n \to R^n$ is a nonlinear function. If there exists a continuous radially unbounded and positive definite function $V(x)$ such that

$$\dot{V}(x) \leq -\alpha V^p - \beta V^q \tag{13}$$

where $\alpha, \beta > 0$, $p > 1$ and $0 < q < 1$, then the origin of this system is globally fixed-time stable with the settling-time T verifying

$$T \leq T_{max} := \frac{1}{\alpha(p-1)} + \frac{1}{\beta(1-q)} \tag{14}$$

i.e., any solution of $\dot{x} = g(t, x), x(0) = 0$ reaches the origin at the fixed settling-time T verifying (14).
Theorem 1 If the control law u_i is designed as in (10), (8) and (7), the reference x_0 is reached in the pre-fixed settling-time $T_{settling}$ verifying

$$T_{settling} \leq max\big(\frac{2^{1.25} + 2^{0.75}\sqrt{n}}{k}, T_0\big) \tag{15}$$

proof For $u_i, i \neq 1$, consider the Lyapunov function defined as follows :

$$V = \frac{1}{2}\sum_{i=1}^{n}(x_i - \tilde{x}_1)^2 \tag{16}$$

The derivative of the Lyapunov function (16) is given as follows:

$$\dot{V} = \sum_{i=1}^{n}(x_i - \tilde{x}_1)(\dot{x}_i - \dot{\tilde{x}}_1) \tag{17}$$

In virtue of (5), (6) and (7), the derivative of the Lyapunov function (17) becomes:

$$\begin{aligned} \dot{V} &= -k\sum_{i=1}^{n}(x_i - \tilde{x}_1)\big(\mid x_i - \tilde{x}_1 \mid^{1/2} + \mid x_i - \tilde{x}_1 \mid^{3/2}\big) \\ &\times \quad sign(x_i - \tilde{x}_1) \\ &= -k\sum_{i=1}^{n}\big(\mid x_i - \tilde{x}_1 \mid^{3/2} + \mid x_i - \tilde{x}_1 \mid^{5/2}\big) \\ &= -k\sum_{i=1}^{n}\big((x_i - \tilde{x}_1)^2\big)^{3/4} + \big((x_i - \tilde{x}_1)^2\big)^{5/4} \end{aligned} \tag{18}$$

Using Lemma 1, yields

$$\begin{aligned} \dot{V} &\leq -k\Big(\sum_{i=1}^{n}(x_i - \tilde{x}_1)^2\Big)^{3/4} - \frac{k}{\sqrt{n}}\Big(\sum_{i=1}^{n}(x_i - \tilde{x}_1)^2\Big)^{5/4} \\ &\leq -k2^{3/4}V^{3/4} - \frac{k2^{5/4}}{\sqrt{n}}V^{5/4} \end{aligned} \tag{19}$$

Thus in virtue of Lemma 2, x_i reaches $\tilde{x}_1$ in the pre-fixed settling-time T_1 verifying

$$\begin{aligned} T_1 &\leq \frac{2^{0.75}\sqrt{n}}{k} + \frac{2^{1.25}}{k} \\ &\leq \frac{2^{1.25} + 2^{0.75}\sqrt{n}}{k} \end{aligned} \tag{20}$$

Thus, for the leader DG (DG1), the settling-time verifies (20), i.e.,

$$T_{settlingDG1} \leq \frac{2^{1.25} + 2^{0.75}\sqrt{n}}{k} \tag{21}$$

For DGi, $i \in \{2, ..., n\}$ since $\tilde{x}_1^i$ reaches x_1 at the fixed-time T_0, then x_i will reach the reference state x_0 in the pre-fixed settling-time $T_{settling}$ verifying

$$T_{settling} \leq max\big(\frac{2^{1.25} + 2^{0.75}\sqrt{n}}{k}, T_0\big) \tag{22}$$

For u_1, the results are straightforward by considering the Lyapunov function $V = \frac{1}{2}\sum_{i=1}^{n}(x_i - x_0)^2$ and following the same previous steps to conclude that the reference state x_0 is reached at the fixed settling-time T_1 verifying (20). Therefore in virtue of (10), the proposed voltage and frequency controllers u_{vi} and $u_{\omega i}$ are given as follows
For voltage control

$$\begin{aligned} u_{v1} &= \int \Big(\dot{V}_0 - k_v\big(\mid V_{1,d} - V_0 \mid^{1/2} + \mid V_{1,d} - V_0 \mid^{3/2}\big) \\ &\times \quad sign(V_{1,d} - V_0) + D_q\dot{Q}_1\Big) \end{aligned} \tag{23}$$

and (for $i \neq 1$)

$$\begin{aligned} u_{vi} &= \int \Big(\dot{\tilde{V}}_1^i - k_v\big(\mid V_{i,d} - \tilde{V}_1^i \mid^{1/2} + \mid V_{i,d} - \tilde{V}_1^i \mid^{3/2}\big) \\ &\times \quad sign(V_{i,d} - \tilde{V}_1^i) + D_q\dot{Q}_i\Big) \end{aligned} \tag{24}$$

For frequency control

$$u_{\omega 1} = \int \Big(\dot{\omega}_0 - k_\omega \big(\mid \omega_{1,d} - \omega_0 \mid^{1/2} + \mid \omega_{1,d} - \omega_0 \mid^{3/2} \big) \times sign(\omega_{1,d} - \omega_0) + D_p \dot{P}_1 \Big)$$

and (for $i \neq 1$)

$$u_{\omega i} = \int \Big(\dot{\tilde{\omega}}_1^i - k_\omega \big(\mid \omega_{i,d} - \tilde{\omega}_1^i \mid^{1/2} + \mid \omega_{i,d} - \tilde{\omega}_1^i \mid^{3/2} \big) \times sign(\omega_{i,d} - \tilde{\omega}_1^i) + D_p \dot{P}_i \Big)$$

where k_v and k_ω are the control gains.

Remark 1 ϵ is the tuning gain of the reference estimation time. The higher ϵ is, the fastest the estimation becomes as indicates (9). However if ϵ is too high, the discontinuous part of the observer will take high values as well and the resulting shattering effect will hinder the leader DG state estimation and the subsequent voltage and frequency control of the microgrid.

Remark 2 For high control performance, it is recommended to tune the control gain ϵ of the observer and the control gains k_v and k_ω of the voltage and frequency controllers to have $T_0 \leq \frac{n\pi}{\epsilon} \leq \frac{2^{1.25}+2^{0.75}\sqrt{n}}{k}$, $k \in \{k_v, k_\omega\}$. In this case, the DGs will have the same settling-time (21) as the leader DG (DG1).

Remark 3 As demonstrated earlier, the proposed controllers achieve fixed-time voltage and frequency reference tracking and disturbances rejection with a model-free design procedure. Also, the basic mathematical operations used in the control formula and the distributed nature of the control system make the numerical implementation of the controller an easy task and reduce the computational burden for the control hardware compared to centralized controllers.

4. COMPARATIVE SIMULATION STUDY

4.1. Simulation presentation

To verify the efficiency of the proposed control approach, its reference tracking performance and its robustness to load power variations will be compared to some of the AC microgrids distributed secondary controllers in the literature that are the voltage controller in [30] and the frequency controller in [28]. The test system is an islanded AC microgrid (Nominal frequency $f_0 = \frac{\omega_0}{2\pi} = 50$ Hz and nominal voltage magnitude $V_0 = 380$V) with four DGs and four loads. The adjacency matrix of the graph modeling the microgrid communication network is $A = \begin{pmatrix} 0000 \\ 1000 \\ 0100 \\ 1000 \end{pmatrix}$. DG1 is the leader node and, thus the only one with access to the reference voltage magnitude $V_0 = 380$V and the reference frequency $f_0 = \frac{\omega_0}{2\pi} = 50$ Hz with the pinning gain $b_1 = 1$ ($b_i = 0$, $i \in \{2, 3, 4\}$ for the other DGs).

The internal voltage and current loops gains and the filter output damping are tuned for high frequency disturbances rejection as follows $K_{pv} = K_{pvi} = 150$, $K_{iv} = K_{ivi} = 250$, $K_{pc} = K_{pci} = 100$, $K_{ic} = K_{ici} = 10$ and $F_i = 0.75 \ \forall i \in \{1, 2, 3, 4\}$. The parameters of the other DGs components are adopted from [31]. . For high control efficiency, the droop coefficients are tuned to limit the voltage drop due to primary control to no more than 2%, which is far less than 10% the maximum deviation tolerated for low voltage networks [34]. The microgrid specifications and the loads active and reactive powers are presented in Table. 1 and Table. 2 respectively.

The control gains k_v and k_ω are set as follows $k_v = k_\omega = 400$. Thus, the regulation and reference tracking settling-time verifies for both voltage and frequency $T_1 \leq 0.014s$. The observer gain is set to $\epsilon = 1131$ in order to have the observer settling-time $T_0 \leq 0.011s < 0.014s$, for better performance as stated in Remark 2. The control system settling-time is then $T_{settling} = 0.014s$. The tuning gains chosen for the controllers in [30] and [28] by the authors of these works are the same used in this paper.

Table 1. The microgrid specifications

	Filter parameters		Droop coefficients		Shunt capacitance	Transformer ratio
DGs	$R_t(m\Omega)$	$L_t(\mu H)$	$D_p \times 10^{-5}$	$D_q \times 10^{-3}$	$C_t(\mu H)$	k
DG1	1.2	93.7	2.08	1.21	62.86	$\frac{0.6}{13.8}$
DG2	1.6	94.8	2.1	1.214	62.86	$\frac{0.6}{13.8}$
DG3	1.5	107.7	2.11	1.217	62.86	$\frac{0.6}{13.8}$
DG4	1.5	90.6	2.12	1.218	62.86	$\frac{0.6}{13.8}$

Table 2. Loads active and reactive powers

	Loads powers	
DGs	P (kW)	Q (kVAR)
DG1	5	2.5
DG2	3	1.5
DG3	5.5	2.75
DG4	4	2

The simulations are conducted considering the following scenario :
1) At $t = 0s$ Beginning of the simulation and application of the primary control where u_{vi} and $u_{\omega i}$ in (3) are as follows

$$u_{vi} = \begin{cases} 380V, For\ DG1 \\ \tilde{V}_1^i, For\ DGi\ i \in \{2, ..., n\} \end{cases} \tag{25}$$

and

$$u_{\omega i} = \begin{cases} 2\pi \times 50Hz, For\ DG1 \\ \tilde{\omega}_1^i, For\ DGi,\ i \in \{2, ..., n\} \end{cases} \tag{26}$$

2) At $t = 0.5s$ Application of the proposed secondary control.
3) At $t = 1.5s$ The powers (active and reactive) of Load 2 decrease.
4) At $t = 2s$ The powers (active and reactive) of Load 4 increase.
5) At $t = 2.5s$ Disconnection of Load1 from the microgrid.
The power variations of the loads are presented respectively in Figure 2 and Figure 3.

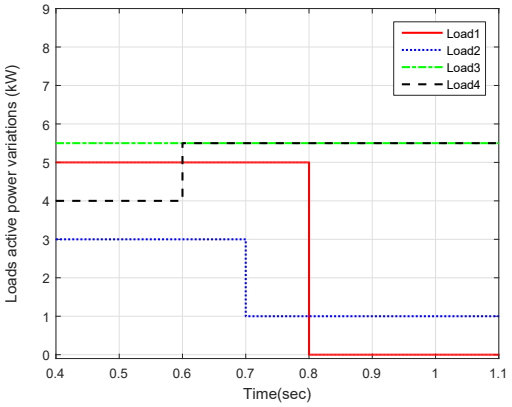

Figure 2. Loads active power consumption (kW)

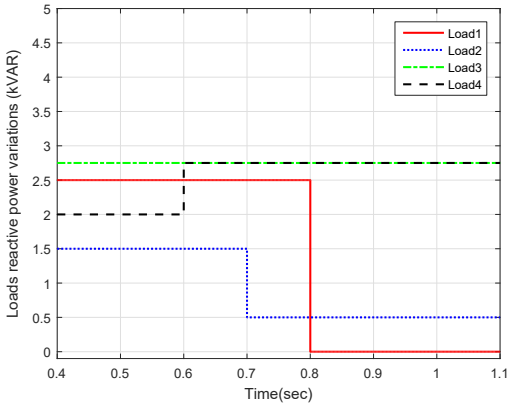

Figure 3. Loads reactive power consumption (kVAR)

4.2. Results and discussion

The results of the simulation are presented in Figure 4, Figure 5 and Figure 6. As seen in Figure 4, the primary droop control maintains voltage and frequency stability yet it yields to steady deviations from the

reference values. When the proposed secondary control is activated at $t = 0.5s$, the four DGs output voltage and frequency are almost instantly restored to their references. The voltage fluctuations caused by loads power variations at $t = 0.8s$, $t = 1.2s$ and $t = 1.6s$ are also rejected to maintain the microgrid voltage at its nominal value with small instantaneous overshoot (less than 6 V). The frequency controller was even more robust as loads power variations didn't cause any disturbances in the microgrid frequency.

Compared to the secondary controller in [30] and [28], as shown in Figure 5 and Figure 6, the designed controller achieves fast frequency and voltage reference restoration before the prefixed settling-time upper bound $0.014s$. Load power variations begin at $t = 0.8s$ as seen in Figure 2 and Figure 3. Figure 5 shows that the proposed voltage control system also rejects the voltage fluctuations before the prefixed settling-time upper bound $0.014s$. The designed fixed-time frequency controller was more robust two external disturbances and maintained the microgrid frequency at its nominal value despite loads power consumption variations, as can be seen in Figure 6. The controllers in [30] and [28] however exhibits slower reference tracking and disturbance rejection dynamics with higher overshoot during load power variations. Increasing the tuning parameters of these controllers will increase the convergence speed but will increase along the overshoot more than the one observed in Figure 5 and Figure 6 and will hinder the system stability and the controller's robustness to parameters uncertainties and external disturbances. The controller suggested in this work, however, achieves the same control objectives in the desired settling-time and with less than 2% overshoot (less than 6 V) which is far less than the maximum allowable voltage deviation 10% [34].

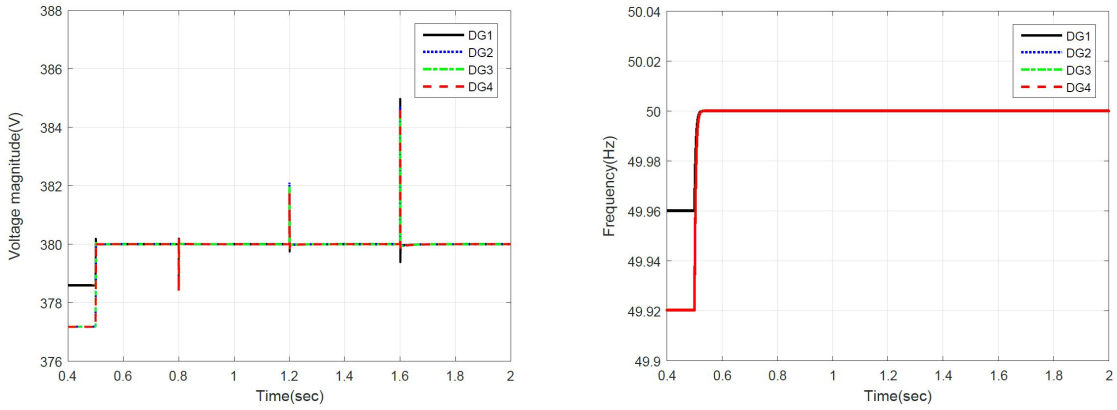

(a) (b)

Figure 4. DGs terminal (a) voltage magnitude (b) frequency

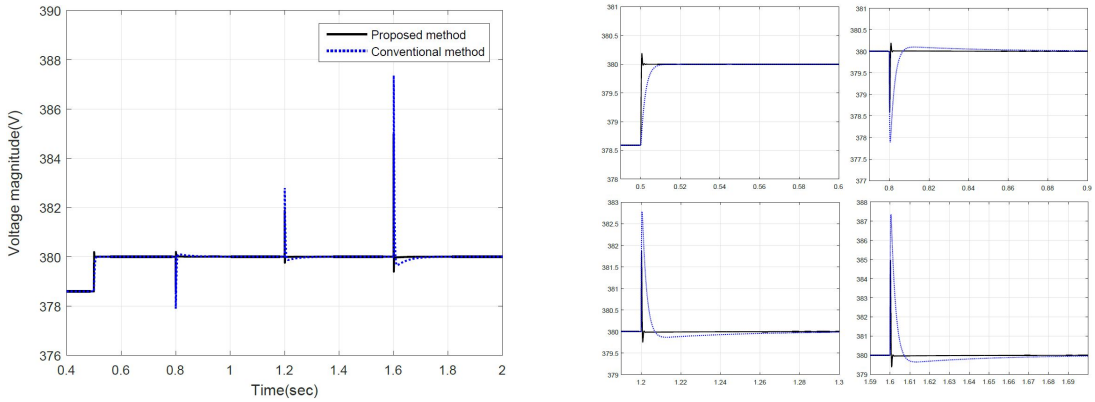

Figure 5. DGs terminal voltage magnitude

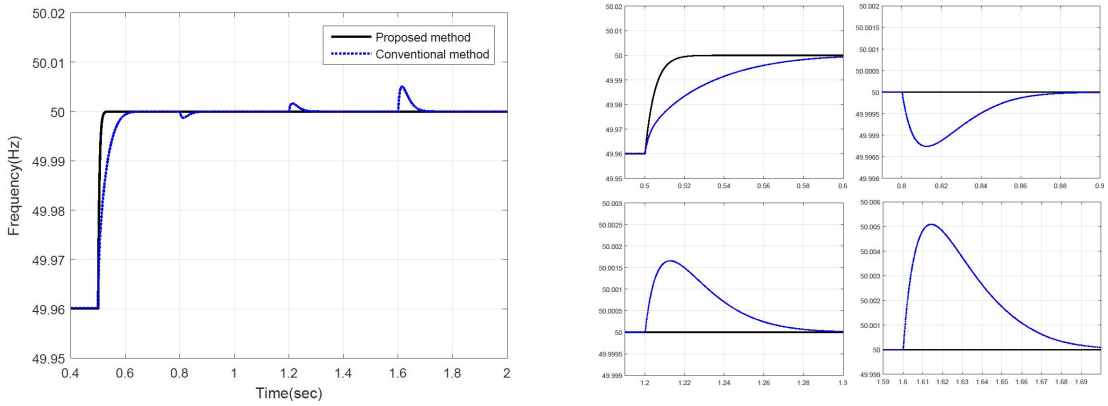

Figure 6. DGs terminal frequency

5. CONCLUSION

In this paper, the problem of voltage and frequency control of distributed generators (DGs) in AC islanded microgrids has been addressed. To obviate the shortcomings of the existing centralized and distributed controllers while providing a better performance, a fixed-time distributed observer-based voltage and frequency secondary control protocol for islanded AC microgrids is proposed. Compared to the existing techniques, a novel fixed-time observer-based feedback-controller is developed in this work for frequency and voltage reference tracking and disturbances rejection before the desired pr-fixed settling-time irrespective to the microgrid initial conditions, parameters uncertainties, the unknown disturbances and without requiring any knowledge of the microgrid topology, parameters, loads or transmission lines impedance for the controller design or tuning. The design of proposed control strategy is also simple, and straightforward and the control law contains simple mathematical operations which means easy numerical implementation and low computational burden for the hardware. The comparative simulations study conducted with some of the conventional microgrids control methods confirmed the theoretical results regarding the controller's performance in voltage and frequency reference tracking and disturbance rejection before at before the desired pre-fixed time, as the suggested control approach exhibited faster reference tracking dynamics and more robustness to load power variations with less overshoot and less reference restorations time.

ACKNOWLEDGEMENT

This work is supported by Morocco's National Center for Scientific and Technical Research within the Research Excellence Scholarships Program.

REFERENCES

[1] J. W. Simpson-Porco, Q. Shafiee, F. Dörfler, J. C. Vasquez, J. M. Guerrero, and F. Bullo, "Secondary Frequency and Voltage Control of Islanded Microgrids via Distributed Averaging," *IEEE Transactions on Industrial Electronics*, vol. 62, no. 11, pp. 7025–7038, Nov. 2015.

[2] Y. Han, K. Zhang, H. Li, E. A. A. Coelho, and J. M. Guerrero, "MAS-Based Distributed Coordinated Control and Optimization in Microgrid and Microgrid Clusters: A Comprehensive Overview," *IEEE Transactions on Power Electronics*, vol. 33, no. 8, pp. 6488–6508, Aug. 2018.

[3] M. Ghazzali, M. Haloua, and F. Giri, "enModeling and Adaptive Control and Power Sharing in Islanded AC Microgrids," *enInt. J. Control Autom. Syst.*, Nov. 2019.

[4] M. Ghazzali and M. Haloua, "Distributed Voltage and Frequency Control of Islanded AC Microgrids," in *2018 6th International Renewable and Sustainable Energy Conference (IRSEC)*, pp. 1–6, Dec. 2018.

[5] T. Qian, Y. Liu, W. H. Zhang, W. H. Tang, and M. shahidehpour, "Event-Triggered Updating Method in Centralized and Distributed Secondary Controls for Islanded Microgrid Restoration," *IEEE Transactions on Smart Grid*, pp. 1–1, 2019.

[6] T. Diep-Thanh, Q. Nguyen-Phung, and H. Nguyen-Duc, "Stochastic control for optimal power flow in islanded microgrid," *Int J Elec & Comp Eng*, vol. 9, no. 2, pp. 1045–1057, Apr. 2019.
[7] G. R. Prudhvi Kumar, D. Sattianadan, and K. Vijaykumar, "A survey on power management strategies of hybrid energy systems in microgrid," *Int J Elec & Comp Eng*, vol. 10, no. 2, pp. 1667–1673, Apr. 2020.
[8] M. R. Basir Khan, J. Pasupuleti, J. Al-Fattah, and M. Tahmasebi, "enEnergy management system for PV-battery microgrid based on model predictive control," *enIndonesian J Elec Eng & Comp Sci*, vol. 15, no. 1, p. 20, Jul. 2019.
[9] Z. Cheng, J. Duan, and M. Chow, "To Centralize or to Distribute: That Is the Question: A Comparison of Advanced Microgrid Management Systems," *IEEE Industrial Electronics Magazine*, vol. 12, no. 1, pp. 6–24, Mar. 2018.
[10] N. L. Díaz, A. C. Luna, J. C. Vasquez, and J. M. Guerrero, "Centralized Control Architecture for Coordination of Distributed Renewable Generation and Energy Storage in Islanded AC Microgrids," *IEEE Transactions on Power Electronics*, vol. 32, no. 7, pp. 5202–5213, Jul. 2017.
[11] M. Karimi, P. Wall, H. Mokhlis, and V. Terzija, "A New Centralized Adaptive Underfrequency Load Shedding Controller for Microgrids Based on a Distribution State Estimator," *IEEE Transactions on Power Delivery*, vol. 32, no. 1, pp. 370–380, Feb. 2017.
[12] N. Srivatchan and P. Rangarajan, "enHalf Cycle Discrete Transformation for Voltage Sag Improvement in an Islanded Microgrid using Dynamic Voltage Restorer," *enInt J Power Electron & Dri Syst*, vol. 9, no. 1, p. 25, Mar. 2018.
[13] M. M. A. Abdelaziz, M. F. Shaaban, H. E. Farag, and E. F. El-Saadany, "A Multistage Centralized Control Scheme for Islanded Microgrids With PEVs," *IEEE Transactions on Sustainable Energy*, vol. 5, no. 3, pp. 927–937, Jul. 2014.
[14] Z. Miao, Y. Liu, Y. Wang, G. Yi, and R. Fierro, "Distributed Estimation and Control for Leader-Following Formations of Nonholonomic Mobile Robots," *IEEE Transactions on Automation Science and Engineering*, vol. 15, no. 4, pp. 1946–1954, Oct. 2018.
[15] A. Marino, "Distributed Adaptive Control of Networked Cooperative Mobile Manipulators," *IEEE Transactions on Control Systems Technology*, vol. 26, no. 5, pp. 1646–1660, Sep. 2018.
[16] S. J. Yoo and B. S. Park, "Connectivity-Preserving Approach for Distributed Adaptive Synchronized Tracking of Networked Uncertain Nonholonomic Mobile Robots," *IEEE Transactions on Cybernetics*, vol. 48, no. 9, pp. 2598–2608, Sep. 2018.
[17] Y. Kantaros and M. M. Zavlanos, "Distributed Intermittent Connectivity Control of Mobile Robot Networks," *IEEE Transactions on Automatic Control*, vol. 62, no. 7, pp. 3109–3121, Jul. 2017.
[18] E. Montijano, E. Cristofalo, D. Zhou, M. Schwager, and C. Sagüés, "Vision-Based Distributed Formation Control Without an External Positioning System," *IEEE Transactions on Robotics*, vol. 32, no. 2, pp. 339–351, Apr. 2016.
[19] F. Mohseni, A. Doustmohammadi, and M. B. Menhaj, "Distributed Receding Horizon Coverage Control for Multiple Mobile Robots," *IEEE Systems Journal*, vol. 10, no. 1, pp. 198–207, Mar. 2016.
[20] W. Yao, J. Liu, and Z. Lu, "Distributed Control for the Modular Multilevel Matrix Converter," *IEEE Transactions on Power Electronics*, vol. 34, no. 4, pp. 3775–3788, Apr. 2019.
[21] P. Wu, Y. Su, J. Shie, and P. Cheng, "A Distributed Control Technique for the Multilevel Cascaded Converter," *IEEE Transactions on Industry Applications*, vol. 55, no. 2, pp. 1649–1657, Mar. 2019.
[22] S. Yang, Y. Tang, and P. Wang, "Distributed Control for a Modular Multilevel Converter," *IEEE Transactions on Power Electronics*, vol. 33, no. 7, pp. 5578–5591, Jul. 2018.
[23] H. Wang, M. Han, J. M. Guerrero, J. C. Vasquez, and B. G. Teshager, "Distributed secondary and tertiary controls for I–V droop-controlled-paralleled DC–DC converters," *Transmission Distribution IET Generation*, vol. 12, no. 7, pp. 1538–1546, 2018.
[24] L. Tarisciotti, G. L. Calzo, A. Gaeta, P. Zanchetta, F. Valencia, and D. Sáez, "A Distributed Model Predictive Control Strategy for Back-to-Back Converters," *IEEE Transactions on Industrial Electronics*, vol. 63, no. 9, pp. 5867–5878, Sep. 2016.
[25] X. Wu, C. Shen, and R. Iravani, "A Distributed, Cooperative Frequency and Voltage Control for Microgrids," *IEEE Transactions on Smart Grid*, vol. 9, no. 4, pp. 2764–2776, Jul. 2018.
[26] X. Lu, X. Yu, J. Lai, Y. Wang, and J. M. Guerrero, "A Novel Distributed Secondary Coordination Control Approach for Islanded Microgrids," *IEEE Transactions on Smart Grid*, vol. 9, no. 4, pp. 2726–2740, Jul. 2018.

[27] A. Bidram, V. Nasirian, A. Davoudi, and F. L. Lewis, *enCooperative Synchronization in Distributed Microgrid Control*, ser. Advances in Industrial Control. Springer International Publishing, 2017.
[28] N. M. Dehkordi, N. Sadati, and M. Hamzeh, "Distributed Robust Finite-Time Secondary Voltage and Frequency Control of Islanded Microgrids," *IEEE Transactions on Power Systems*, vol. 32, no. 5, pp. 3648–3659, Sep. 2017.
[29] A. Bidram, A. Davoudi, F. L. Lewis, and J. M. Guerrero, "Distributed Cooperative Secondary Control of Microgrids Using Feedback Linearization," *IEEE Transactions on Power Systems*, vol. 28, no. 3, pp. 3462–3470, Aug. 2013.
[30] A. Bidram, A. Davoudi, F. L. Lewis, and Z. Qu, "Secondary control of microgrids based on distributed cooperative control of multi-agent systems," *Transmission Distribution IET Generation*, vol. 7, no. 8, pp. 822–831, Aug. 2013.
[31] M. S. Sadabadi, Q. Shafiee, and A. Karimi, "Plug-and-Play Voltage Stabilization in Inverter-Interfaced Microgrids via a Robust Control Strategy," *IEEE Transactions on Control Systems Technology*, vol. 25, no. 3, pp. 781–791, May 2017.
[32] Z. Zuo, B. Tian, M. Defoort, and Z. Ding, "Fixed-Time Consensus Tracking for Multiagent Systems With High-Order Integrator Dynamics," *IEEE Transactions on Automatic Control*, vol. 63, no. 2, pp. 563–570, Feb. 2018.
[33] Z. Zuo, "Nonsingular fixed-time consensus tracking for second-order multi-agent networks," *Automatica*, vol. 54, pp. 305–309, Apr. 2015.
[34] C. Moldovan, C. Damian, and O. Georgescu, "Voltage Level Increase in Low Voltage Networks through Reactive Power Compensation Using Capacitors," *Procedia Engineering*, vol. 181, pp. 731–737, Jan. 2017.